Service restoration based on AMI and networked MGs under extreme weather events

Zhaoyu Wang[1] ✉, Jianhui Wang[2]

[1]Department of Electrical and Computer Engineering, Iowa State University, 2520 Osborn Drive, Ames, IA 50011, USA
[2]Division of Decision and Information Sciences, Argonne National Laboratory, Argonne, IL 60439, USA
✉ E-mail: wzy@iastate.edu

Abstract: This study proposes a comprehensive power outage detection and service restoration framework for a distribution system with advanced metering infrastructure (AMI) meters and networked microgrids (MGs). To cope with the resilience challenge of communication networks in severe weather events, the authors propose a decentralised outage detection method which obtains the total number of customers and the total amount of lost load in the outage area via local information exchanges among AMI meters. To provide fast-response service restoration, the proposed framework incorporates the network reconfiguration and the local power support from the connected MGs. The optimal restoration problem is formulated as a mixed-integer quadratic programme that controls distributed generators and loads in MGs and line switches to maximise the restored critical loads. Case studies on a modified 69-bus distribution system with networked MGs demonstrate the effectiveness of the proposed methodology in both outage detection and service restoration.

Nomenclature

B	set of buses
B^S	subset of buses that are substations
B^G	subset of buses with microgrids
L	set of lines
L^S	subset of lines B^S with switches
L^F	subset of on-fault lines
W	set of nodes with DGs in microgrids
N	set of nodes with loads in microgrids
i, j	index for buses in primary network
k	index for buses in secondary network
t	index for time
n	index for nodes with loads in microgrids
w	index for nodes with DGs in microgrids
l	iteration step in consensus algorithm
r	line resistance
x	line reactance
p^d	active load consumption at a node in secondary distribution network/MG
K_i	total number of consumers in the ith secondary distribution network
c^s	cost of switch operation
c^D	cost of load shedding (priority index of a load)
c^g	generation cost of a micro-turbine
p^{wt}/p^{pv}	predicted active power output of a wind turbine/photovoltaic generator
M	disjunctive parameter
S^{Lmax}	maximum line capacity
S^{Gmax}	maximum generation capacity
ε	maximum allowed voltage deviation
$P^{dch,\,max}/P^{ch,\,max}$	maximum discharging/charging
EC	capacity of the energy storage
ψ_d/ψ_c	discharging/charging efficiency
T	time interval between t and $t-1$
τ	step size in consensus algorithm
γ	connection status of a consumer
μ	total number of on-outage AMI meters
η	total number of meters with malfunction/planned outage/no-pay disconnection
V	voltage magnitude
P	active power flow
Q	reactive power flow
P^D	active load consumption at a bus in primary distribution network
Q^D	reactive load consumption at a bus in primary distribution network
p^{mt}/q^{mt}	active/reactive power output of a micro-turbine
p^{es}	charging/discharging of ESS
α/β	discharging/charging state of ESS
SOC	state-of-charge of ESS
u^D	binary variable of load connection status in primary distribution network
u^M	binary variable of load connection status in microgrids
z	binary indicator of line flow direction
y	binary indicator of line switch status
X	iteration variables

1 Introduction

Fault location, isolation and service restoration (FLISR) is one of the major functions of a distribution management system. An efficient FLISR can dramatically decrease the duration and number of customers affected by outages [1]. Massive power outages in severe weather events cause significant damage to economy and society, which is the driving force to develop a fast and accurate system for outage location and service restoration.

In traditional distribution grids, outage locating is a manually intensive, complicated and time-consuming process. Distribution supervisory control and data acquisition provides more operation information at the lower levels of a distribution grid such as distribution transformers and fuses. In recent years, the implementation of advanced metering infrastructure (AMI) offers further visibility to the secondary distribution networks and consumers. These monitoring systems can provide real-time and accurate information, which can be used to improve the outage detection and location. For example, the study in [2] proposed a knowledge-based system to locate distribution system outages

using data from customer trouble calls and wireless automated meter reading systems; Chen *et al.* [3] developed a fuzzy Petri nets-based method to detect fraudulent consumption and power outages using AMI data. However, the existing meter-based detection methods require a centralised communication infrastructure which is costly and unreliable.

After on-outage areas are detected and located, utilities will conduct service restoration. Many studies have been performed in distribution grid restoration. Reference [4] proposed a service restoration algorithm based on network reconfiguration and capacitor control. The multi-objective optimisation problem is solved by a heuristic algorithm. Toune *et al.* in [5] compared the performance of genetic algorithm, parallel simulated annealing, tabu search and reactive tabu search in solving the optimal service restoration problem. The study in [6] presented a rule-based expert system with a coloured Petri net inference model to find the optimal switching operation for the distribution system restoration. Priority indices are assigned to each feeder and service zone. Reference [7] proposed a two-step restoration scheme for multiple faults with the first step to set up a plan one by one for each outage region and the second step to find a new feasible configuration for the entire system. Kumar *et al.* in [8] applied a non-dominated sorting genetic algorithm to solve the multi-objective service restoration problem considering priority customers, and remotely controlled as well as manually controlled switches. The objectives are to minimise the out-of-service area, number of switch operations and power losses. Traditional service restoration is based on reconfiguration, which is slow, constrained by capacity limits, and depends on the availability of switches. In an extreme weather event, multiple faults may happen in a distribution system, which adds more challenges to the reconfiguration to find a feasible topology. The integration of distributed generators (DGs) and microgrids (MGs) makes it possible to realise fast-response service restoration by using local self-healing techniques.

MGs are active energy systems comprised of DGs, energy storage systems (ESSs) and controllable loads via demand response (DR) programmes. A modern distribution system may consist of multiple MGs to improve the operation, reliability and economic benefits [9]. After an outage is detected and located, MGs can be controlled to quickly provide local restoration capacity to assist the service restoration process. Recently, there are studies on leveraging MGs/DGs to facilitate service restoration and improve grid resilience. Wang *et al.* in [10] reviewed the research on forecasting natural disaster-related power system disturbances and performing service restoration. Reference [11] proposed a spanning tree search-based restoration strategy incorporating MGs. However, the outage detection and dispatches of DGs and controllable loads are not discussed. The study in [12] presented a method to sectionalise the on-outage portion of a power distribution system into multiple MGs to increase the grid resilience. Reference [13] studied the service restoration in an islanded MG after a blackout. The authors developed control algorithms to black start an MG, which is different from our objective to leverage MGs to restore their connected distribution system. Chen *et al.* in [14] developed an operation approach by forming multiple MGs energised by DGs from the radial distribution system in real-time operations, to restore critical loads from the power outage. In [15], a transformative architecture is designed for the self-healing of networked MGs, in which MGs can support and interchange electricity with each other in a decentralised way. In [16], Ansari and Mohagheghi presented a restoration strategy to alleviate the congestion on the restoration path by increasing DG generation and/or islanding MGs. However, the outage detection and system reconfiguration are not included.

The purpose of this paper is to design a comprehensive outage detection, location and service restoration strategy based on AMI meters and MGs to make distribution grids more resilient to large weather events. AMI is usually installed at the consumer level, which makes it a rich source of data on what is occurring within a distribution system. However, it is challenging for the control centre to process the large amount of data sent by AMI in a fast,

reliable and resilient way. The challenge becomes more severe in an extreme weather event when communication infrastructures are wrecked and a high volume of service requests are issued. To solve this difficulty, this paper proposes a decentralised outage locating system. In a certain secondary distribution network, an AMI meter only communicates with its neighbouring counterparts. A routing meter aggregates information using a consensus algorithm [17, 18]. The routing meter filters out meaningless data and report useful aggregated information to the central controller. If the routing meter is down, a new routing meter will be automatically selected from its neighbouring meters. Compared with existing centralised frameworks, the proposed decentralised method has many advantages such as lower complexity for communication and computation, and more reliable and robust, i.e. free of a single point failure. For the service restoration, this paper proposes a self-healing strategy based on MGs and reconfiguration. MGs reschedule the dispatchable-DGs, ESSs and DR loads to provide local power support to the on-outage areas. The proposed comprehensive framework can achieve fast and reliable outage location and service restoration, thus improving the grid resilience under extreme weather events.

The major contributions of this paper are summarised as follows:

- A completely decentralised outage detection method based on AMI meters.
- An optimal service restoration method incorporating MGs, DGs, load curtailment and reconfiguration.

The remainder of this paper is organised as follows. Section 3 presents the decentralised outage detection and location method based on AMI. Section 4 introduces the mathematical model for the optimal service restoration based on MGs. In Section 5, the numerical results on a test distribution system with multiple MGs are provided. Section 6 concludes this paper with the major findings.

2 Decentralised outage detection and location based on AMI

Fig. 1 shows examples of primary and secondary power distribution systems with multiple MGs. We assume that AMI meters are fully deployed in the system, i.e. all consumers in the secondary distribution system are equipped with AMI meters. These meters are communicated through wireless networks, and there is a gateway that collects all meters' measurements at the substation and communicates with the control centre through optical fibre cables [19].

A major challenge is to effectively collect the operation information from all customers (e.g. the connection status and the aggregated power consumption) to make optimal decisions for service restoration. In each secondary distribution network, there is a routing AMI meter which can conduct the function of a regular meter and communicate with the control centre. All regular AMI meters do not communicate with the control centre directly, but exchange information with their neighbouring counterparts (and the routing AMI meter) in the same secondary distribution network iteratively through wireless communications. The exchanged information includes the power consumption and connection status. The routing meter calculates the aggregated information of all meters in a decentralised way, and within a certain number of iterations, the global information (e.g. the total number of on-outage consumers and the aggregated last-read power consumption of these consumers) is known to the routing meter. In this way, the proposed decentralised outage detection method is more reliable and resilient than centralised ones since a single point of coupling is not needed. The above communication structure is known to be a meshed communication technology which has been implemented in smart meter systems [19].

Let $\gamma_{i,k,t}$ represent the connection status of consumer k in the ith secondary distribution system connected with the bus i of the primary distribution network. Here, $\gamma_{i,k,t} = 0$ indicates the normal
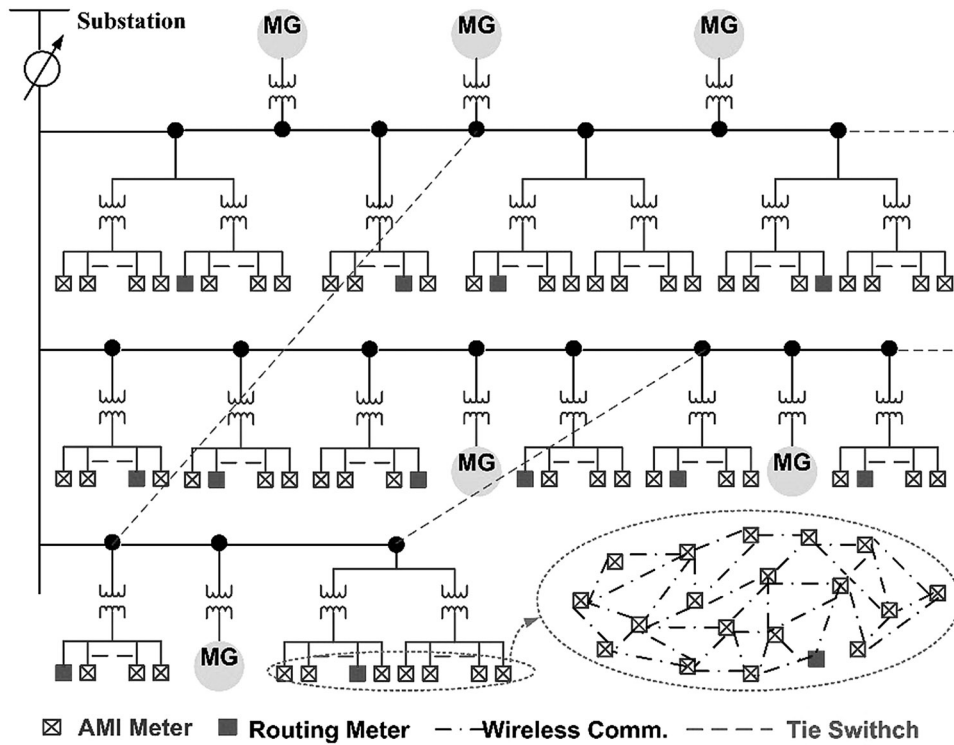
Fig. 1 *Distribution system with networked MGs*

operation and $\gamma_{i,k,t} = 1$ means there is an outage/malfunction with the corresponding meter. Every AMI meter exchanges $\gamma_{i,k,t}$ and $p_{i,k,t}^{\mathrm{d}}$ with its neighbouring counterparts. We assume that the number of AMI meters (customers) in the ith secondary distribution system is K_i, which is known to the routing meter through broadcasting [20]. The average value of connection status in the ith secondary distribution system is

$$\bar{\gamma}_{i,t} = \frac{1}{K_i} \sum_{k=1}^{K_i} \gamma_{i,k,t} \tag{1}$$

From the definition of $\gamma_{i,k,t}$, we know that the total number of on-outage/malfunction meters in the ith secondary distribution system is

$$\mu_{i,t} = \bar{\gamma}_{i,t} K_i \tag{2}$$

As shown in Fig. 2, when a meter detects an outage, it decides whether it is momentary or permanent. Then it exchanges information with peer meters. The routing meter calculates the aggregated power consumption and the number of on-outage meters based on an average consensus algorithm. It is assumed that the routing meter in the ith secondary distribution network has received a list of $\eta_{i,t}$ meters under communication failure, planned outage and no-pay disconnection from the central controller through broadcasting. In other words, the central controller assumes these $\eta_{i,t}$ meters are not working properly. If $\mu_{i,t} - \eta_{i,t}$ is small, e.g. only one or two customers lost power in the ith secondary distribution network, the routing meter will request the IDs of these customers without initiating a service restoration. If $\mu_{i,t} - \eta_{i,t}$ is larger than a critical value μ_{c}, a major outage is reported to the control centre and a service restoration is requested. Here, μ_{c} can be determined by system operators based on the following considerations: (i) historical outage data, e.g. the typical outage sizes; (ii) the loading condition, e.g. compared with normal load consumption, how much load has been lost; and (iii) the operation states of transformers and automatic switches.

At time t, the average load consumption at bus i is

$$\bar{P}_{i,t}^{\mathrm{D}} = \frac{1}{K_i} \sum_{k=1}^{K_i} p_{i,k,t}^{\mathrm{d}} \tag{3}$$

It is assumed that customers in the same secondary network have the same load priority. Hence, the aggregated power consumption of consumers connected with the bus i can be calculated as

$$P_{i,t}^{\mathrm{D}} = \bar{P}_{i,t}^{\mathrm{D}} K_i \tag{4}$$

The aggregated last-read power consumption of the on-outage meters will also be reported to the central controller to assist making the restoration plan. Both $\bar{\gamma}_{i,t}$ and $\bar{P}_{i,t}^{\mathrm{D}}$ can be obtained from the average consensus algorithm [17, 20], which computes the average value of all entities iteratively using only local information exchange. In the consensus algorithm, the iteration variable can be linearly updated as follows

$$X_{i,k,t}(l+1) = X_{i,k,t}(l) + \tau \cdot \sum_{a \in A_i} (X_{i,a,t}(l) - X_{i,k,t}(l)) \tag{5}$$

where $X_{i,k,t}$ represents the vectors of $\gamma_{i,k,t}$ and $p_{i,k,t}^{\mathrm{d}}$ for a meter at the lth step, A_i represents the set of its connected neighbouring meters. $X_{i,k,t}(l)$ will converge to the average of initialised values of all meters in the same secondary distribution network. For example, if the initial value of $X_{i,k,t}$ is set as $X_{i,k,t}(0) = \gamma_{i,k,t}$, then the value of $X_{i,k,t}(l)$ will converge to the average value $(1/K_i) \sum_k \gamma_{i,k,t}$ with a proper step size. $(1/K_i) \sum_k p_{i,k,t}^{\mathrm{d}}$ can be calculated in the same way. The convergence of the average consensus algorithm has been extensively studied in the literature [18] and is not a focus of this paper. In brief, the convergence is related to the eigenvalues of the Laplacian matrix representing the communication network. The step size that results in the minimum convergence time can be calculated as $\tau = 2/[\varphi_2(\boldsymbol{L}) + \varphi_K(\boldsymbol{L})]$, where $\varphi_2(\boldsymbol{L})$ and $\varphi_K(\boldsymbol{L})$ represent the second and the kth smallest eigenvalues of the graph Laplacian matrix $\boldsymbol{L}$. In extreme weather events, the communication infrastructure maybe damaged and
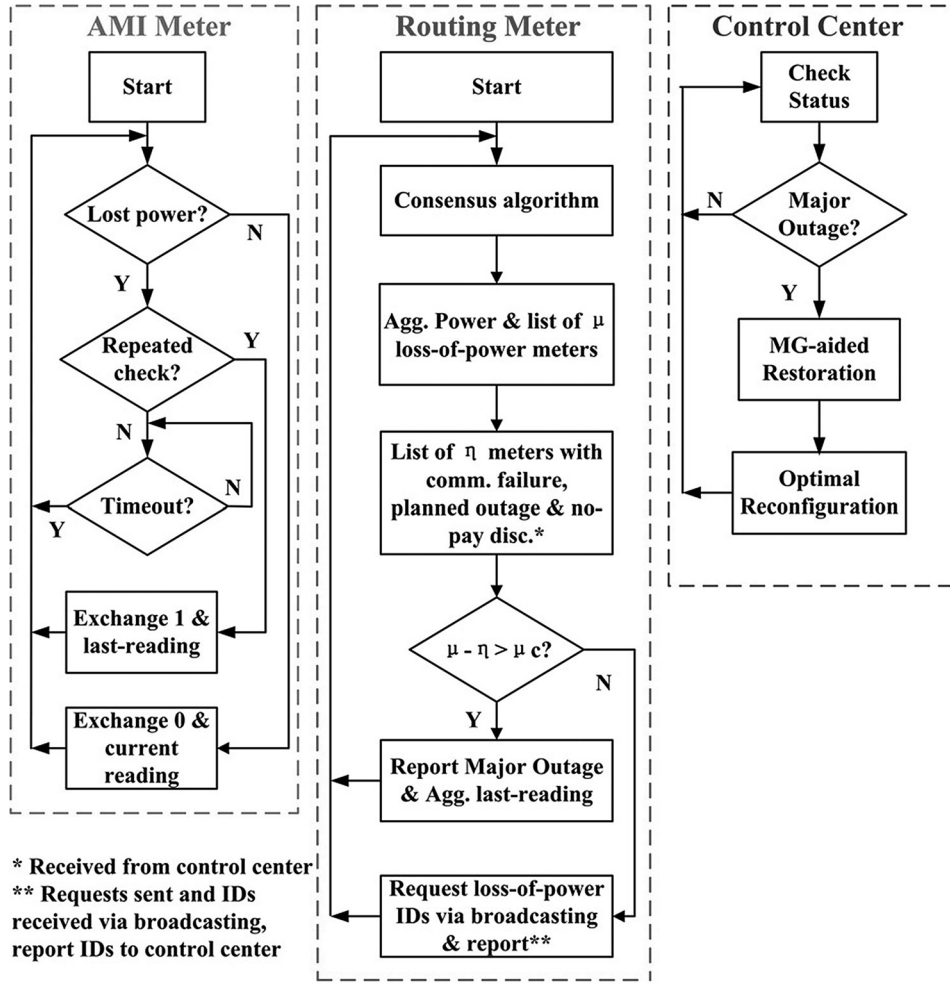
Fig. 2 *Flowchart of the proposed method*

needs to be formed in a dynamic manner [14]. The topology of the network can be designed using the convergence features. The dynamic formation of the communication network is out of the scope of this paper.

3 Mathematical modelling of service restoration

This section introduces a widely used distribution grid model and provides the formulation for optimal service restoration based on multiple MGs.

3.1 Distribution grid model

DistFlow equations are used in this paper to calculate complex power flows in a distribution grid [21, 22]. DistFlow equations can be defined as follows

$$\sum_{j:(i,j)\in L} P_{j,i} = P_{i,j} + \frac{r_{i,j}(P_{i,j}^2 + Q_{i,j}^2)}{V_j^2} + P_i^{\mathrm{D}} \quad (6)$$

$$\sum_{j:(i,j)\in L} Q_{j,i} = Q_{i,j} + \frac{x_{i,j}(P_{i,j}^2 + Q_{i,j}^2)}{V_j^2} + Q_i^{\mathrm{D}} \quad (7)$$

$$V_j^2 = V_i^2 - 2(r_{i,j}P_{i,j} + x_{i,j}Q_{i,j}) + \frac{(r_{i,j}^2 + x_{i,j}^2)(P_{i,j}^2 + Q_{i,j}^2)}{V_j^2} \quad (8)$$

Note $P_{i,j}$ and $Q_{i,j}$ are different from $P_{j,i}$ and $Q_{j,i}$. The DistFlow equations can be simplified by dropping all quadratic terms. The linearised power flow equations have been extensively used and justified in both traditional distribution systems and MGs [21, 23]

$$\sum_{j:(i,j)\in L} P_{j,i} = P_{i,j} + P_i^{\mathrm{D}} \quad (9)$$

$$\sum_{j:(i,j)\in L} Q_{j,i} = Q_{i,j} + Q_i^{\mathrm{D}} \quad (10)$$

$$V_j = V_i - \frac{r_{i,j}P_{i,j} + x_{i,j}Q_{i,j}}{V_0^2} \quad (11)$$

3.2 Optimisation problem for service restoration based on MGs

After locating the outage, service restoration is expected to pick up loads in the affected areas. Reconfiguration is the prime way to perform restoration in traditional distribution grids. However, it suffers from many constraints such as the availability and limited operations of switches, and capacity limits of transformers and lines. In this paper, the power support from local MGs is used to restore the on-outage loads. To provide enough power support to pick up the maximum loads under outage, an MG should increase its DG outputs and curtail non-critical loads within the MG. The general optimisation problem for the service restoration with

multiple MGs can be formulated as follows

$$
\min \sum_{(i,j)\in L^S} c^S |y_{i,j} - y_{i,j}^0| + \sum_t \left(\sum_{i\in B, k\in K} c_i^D (1 - u_{i,t}^D) P_{i,t}^D \right.
$$

$$
\left. + \sum_{i\in B^G, n\in N} c_{i,n}^D (1 - u_{i,n,t}^M) p_{i,n,t}^d + \sum_{i\in B^G, w\in W} c_{i,w}^g p_{i,w,t}^{mt} \right) \quad (12)
$$

$$
\text{s.t.} \quad \sum_{j:(i,j)\in L} P_{j,i,t} = P_{i,j,t} + u_{i,t}^D P_{i,t}^D, \quad \forall i \in B \backslash \{B^S \cup B^G\} \quad (13)
$$

$$
\sum_{j:(i,j)\in L} Q_{j,i,t} = Q_{i,j,t} + u_{i,t}^D Q_{i,t}^D, \quad \forall i \in B \backslash \{B^S \cup B^G\} \quad (14)
$$

$$
\sum_{j:(i,j)\in L} P_{j,i,t} = P_{i,j,t} + u_{i,t}^D P_{i,t}^D - P_{i,t}^G, \quad \forall i \in \{B \cap B^G\}\backslash B^S \quad (15)
$$

$$
\sum_{j:(i,j)\in L} Q_{j,i,t} = Q_{i,j,t} + u_{i,t}^D Q_{i,t}^D - Q_{i,t}^G, \quad \forall i \in \{B \cap B^G\}\backslash B^S \quad (16)
$$

$$
P_{i,t}^G = \sum_w (p_{i,w,t}^{mt} + p_{i,w,t}^{wt} + p_{i,w,t}^{pv} + p_{i,w,t}^{es}) - \sum_n u_{i,n,t}^M p_{i,n,t}^d,
$$

$$
\forall i \in B^G, \quad w \in W, \quad n \in N \quad (17)
$$

$$
Q_{i,t}^G = \sum_w q_{i,w,t}^{mt} - \sum_n u_{i,n,t}^M q_{i,n,t}^d,
$$

$$
\forall i \in B^G, \quad w \in W, \quad n \in N \quad (18)
$$

$$
0 \le P_{i,j,t} \le Mz_{i,j,t}, \quad \forall i, j \in B \quad (19)
$$

$$
0 \le Q_{i,j,t} \le Mz_{i,j,t}, \quad \forall i, j \in B \quad (20)
$$

$$
z_{i,j,t} \ge 0, \quad \forall j \in B \backslash B^S \quad (21)
$$

$$
z_{i,j,t} = 0, \quad \forall j \in B^S \quad (22)
$$

$$
z_{i,j,t} + z_{j,i,t} = 1, \quad (i,j) \in L\backslash\{L^S \cup L^F\} \quad (23)
$$

$$
z_{i,j,t} + z_{j,i,t} = y_{i,j,t}, \quad \forall (i,j) \in L^S \quad (24)
$$

$$
z_{i,j,t} + z_{j,i,t} = 0, \quad \forall (i,j) \in L^F \quad (25)
$$

$$
\sum_{j:(i,j)\in L} z_{j,i,t} = 1, \quad \forall (i,j) \in L^S \quad (26)
$$

$$
V_{j,t} \ge V_{i,t} - \frac{r_{i,j}P_{i,j,t} + x_i Q_{i,j,t}}{V_0} - M(1 - z_{i,j,t}), \quad \forall i, j \in B \quad (27)
$$

$$
V_{j,t} \le V_{i,t} - \frac{r_{i,j}P_{i,j,t} + x_i Q_{i,j,t}}{V_0} + M(1 - z_{i,j,t}), \quad \forall i, j \in B \quad (28)
$$

$$
1 - \varepsilon \le V_{i,t} \le 1 + \varepsilon, \quad \forall i \in B \quad (29)
$$

$$
V_{i,t} = 1, \quad \forall i \in B^S \quad (30)
$$

$$
(P_{i,j,t})^2 + (Q_{i,j,t})^2 \le (S_{i,j}^{Lmax})^2, \quad \forall (i,j) \in L \quad (31)
$$

$$
(p_{i,w,t}^{mt})^2 + (q_{i,w,t}^{mt})^2 \le (S_{i,w}^{Gmax})^2, \quad \forall i \in B^G, \quad w \in W \quad (32)
$$

$$
-p_{i,w}^{ch,max}\beta_{i,w,t} \le p_{i,w,t}^{es} \le P_{i,w}^{dch,max}\alpha_{i,w,t}, \quad \forall i \in B^G, \quad w \in W \quad (33)
$$

$$
0 \le \alpha_{i,w,t} + \beta_{i,w,t} \le 1, \quad \forall i \in B^G, \quad w \in W \quad (34)
$$

$$
SOC_{i,w,t} = SOC_{i,w,t-1} - T(\alpha_{i,w,t}p_{i,w,t}^{es}\psi_d^{-1} + \beta_{i,w,t}p_{i,w,t}^{es}\psi_c)/EC_{i,w},
$$

$$
\forall i \in B^G, \quad w \in W \quad (35)
$$

$$
SOC_{i,w}^{min} \le SOC_{i,w,t} \le SOC_{i,w}^{max}, \quad \forall i \in B^G, \quad w \in W \quad (36)
$$

$$
u_{i,t}^D, u_{i,n,t}^M, z_{i,j,t}, y_{i,j}, \alpha_{i,w,t}, \beta_{i,w,t} \in \{0, 1\} \quad (37)
$$

In the above formulation, the objective function (12) represents costs of switching actions of sectionalising switches, load shedding in the distribution grid and MGs and the power generation. The first item in the objective function calculates the number of opening/closing actions by comparing the current status of the switches to the corresponding initial status. Since y is a binary variable, i.e. $y^2 = y$, the absolute value operator in the first item can be replaced by a square operator. Thus, the first item in the objective function can be linearised as

$$
\sum_{(i,j)\in L^S} \left| y_{i,j} - y_{i,j}^0 \right| = \sum_{(i,j)\in L^S} (y_{i,j} - y_{i,j}^0)^2
$$

$$
= \sum_{(i,j)\in L^S} (y_{i,j} + y_{i,j}^0 - 2y_{i,j}y_{i,j}^0) \quad (38)
$$

The second and third items represent the costs of load shedding in the distribution grid and MGs, respectively. For an on-outage area, $u^D = 1$ indicates that the corresponding load is picked up in the restoration. The last item represents the generation cost of micro turbines (MTs). It is assumed that the generation costs of wind turbine (WT), photovoltaics (PVs) and ESSs can be neglected [24]. c^s, c^D and c^g are used to convert the objectives to be monetary values. Moreover, larger values of c^D can be assigned to loads with a higher priority.

Constraints (13)–(16) represent the power balance equations in the linearised DistFlow method, in which (13) and (14) are for buses without MGs and (15) and (16) are for buses with MGs. The aggregated load consumption at the bus i can be obtained from the decentralised information exchange among AMI meters as discussed in Section 3. Constraints (17) and (18) represent the active and reactive power support from an MG to its connected bus, respectively. Loads in an MG can be shed to support high-priority loads in the distribution grid. It is assumed that only the controllable DGs, i.e. MTs in this paper, can inject reactive power to the grid [25]. In constraints (19)–(23), $z_{i,j}$ and $z_{j,i}$ denote which direction, if any, the power flow can travel. For example, if $z_{i,j} = 0$, then $P_{i,j} = 0$ and $Q_{i,j} = 0$ by (19) and (20) and $z_{j,i} = 1$ by (23). This means power flows from bus j to bus i. Constraint (23) is for a line without a sectionalising switch. For a line with a switch, we use a binary variable $y_{i,j}$ to describe the open/closed status of the line switch as shown in constraint (24). In constraint (25), the line flow is always zero if the line is on fault. Note that $z_{i,j}$ is directional and $y_{i,j}$ is not directional. Constraints (27) and (28) reproduce (11) in the linearised DistFlow method when $z_{i,j} = 1$, and become redundant when $z_{i,j} = 0$. The radial topology of network can be guaranteed by constraints (21)–(26). The detailed descriptions can be found in [22]. Constraint (29) guarantees that the voltage level of each node is within a predefined range, ε is usually set to be 0.05. In constraint (30), the voltage level at the substation is set to be 1 pu. Constraint (31) describes the line flow limits. Constraint (32) guarantees the output of an MT is within its capacity. Constraint (33) represents the charging and discharging limits of an ESS according to its operation mode. For example, $\alpha = 1$ and $\beta = 0$ represents the discharging mode of the ESS and the maximum discharging limits are imposed. Constraint (34) guarantees that the ESS works in only one mode at a certain time. Constraint (35) represents the state-of-charge (SOC) of an ESS. Constraint (36) represents the limit of SOC.

The above formulation is a mix-integer quadratic programming problem and can be solved by commercial solvers such as GAMS/DICOPT [26].

4 Numerical results

As shown in Fig. 3, a modified 69-bus distribution system with multiple MGs is used in this paper. Details about the 69-bus test system can be found in [27]. Fig. 4a shows the configuration of a secondary distribution system, which is assumed to be the same to all secondary systems. The numbers of customers in the secondary systems are listed in Table 1. It is assumed that all MGs share the same topology as shown in Fig. 4b. The sizes of a wind turbine, a micro-turbine, a PV generator and an ESS are set to be 100, 250, 50 and 50 kW, respectively. The energy capacity of ESS is set to be 250 kWh. The line resistance and reactance of all MGs are set to be 0.008 and 0.0012 Ω, respectively.

The multipliers, as shown in Table 2, are used to make the load profiles and predicted DG outputs change with time. Without loss of generality, it is assumed that the multipliers of all nodes are the same. The predicted loads and renewable DG outputs are products of the basic components and the multipliers. The basic component for a DG is assumed to be its size. The values of basic load of the 69-bus distribution system (the primary distribution system) can be found in [27] and the basic load for each MG node is set to be 20 kW. As shown in Table 3, loads are classified into two categories: critical loads and normal loads. For an MG, it is assumed that 70% of the loads are critical. Note the above parameter settings are for illustration, system operators can change the settings according to the practical systems and information.

A severe weather event may result in multiple faults. Therefore, we consider a scenario with six faults that are randomly located as shown in Table 4. We assume that faults happen at the peak time 17:15 and last about 5 h to 22:00 [28]. Take the secondary distribution system connected with bus 21 as an example to show the effectiveness of the proposed decentralised fault detection. There are 40 customers in the secondary distribution network as shown in
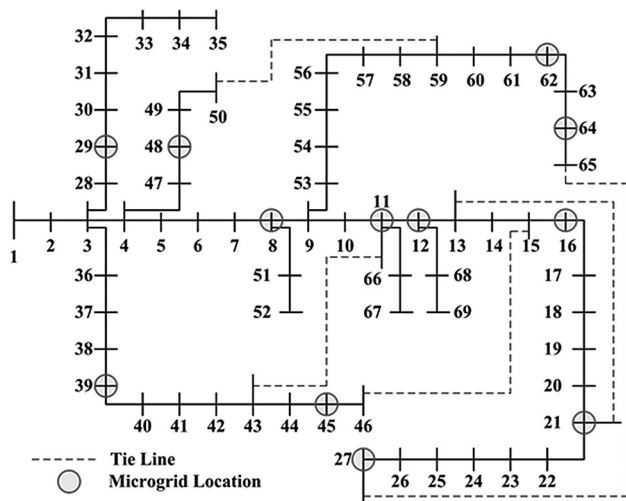

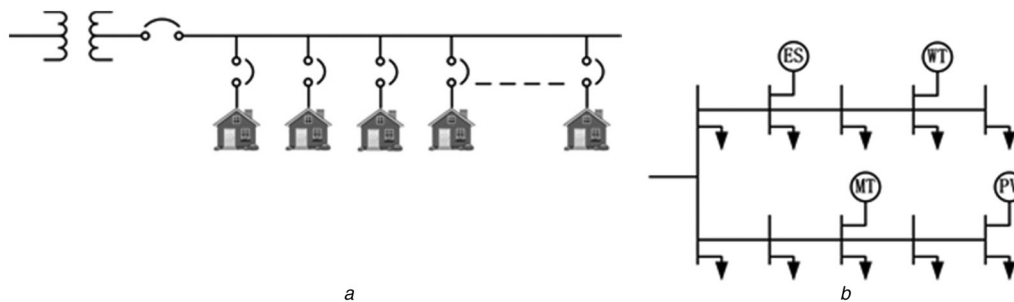**Fig. 3** *Test distribution system with networked MGs*

Fig. 4 *Numerical results*
a Secondary distribution system
b Topology of an MG

Table 1 Numbers of customers in secondary distribution systems

Bus number in primary system	Number of customers in secondary system
2, 3, 4, 5, 15, 19, 23, 25, 30, 31, 32, 38, 42, 44, 47, 56, 57, 58, 60, 63	0
6, 20, 41	1
13, 14, 22, 35, 43, 52, 53	2
26, 27, 33	4
34, 66, 67	6
39, 40, 45, 55	8
9, 10, 24, 28, 29, 36, 37, 62, 68, 69	10
7, 16, 45, 46, 51	15
17, 18, 65	20
8, 48, 59	30
11, 12, 21	40
64	80
49, 50	120
61	400

Table 2 Load and generation multipliers

Time	Active load multiplier	Reactive load multiplier	Wind power multiplier	Solar power multiplier
17:00	0.9935	0.9821	0.2937	0.1050
17:15	1.000	1.000	0.2934	0.0604
17:30	0.9897	0.9565	0.2972	0.0603
17:45	0.9949	0.9423	0.2988	0.0531
18:00	0.9968	0.9634	0.2944	0.0527
18:15	0.9894	0.9256	0.3030	0.0518
18:30	0.9514	0.8967	0.3252	0.0494
18:45	0.9637	0.9218	0.3139	0.0494
19:00	0.9858	0.9071	0.3142	0.0432
19:15	0.9465	0.8934	0.3260	0.0420
19:30	0.9208	0.8884	0.3203	0.0322
19:45	0.9343	0.8886	0.3237	0.0411
20:00	0.9231	0.8909	0.3227	0.0400
20:15	0.8839	0.8843	0.3178	0.0150
20:30	0.8781	0.8791	0.3283	0.0116
20:45	0.8742	0.8830	0.3345	0.0135
21:00	0.8687	0.8829	0.3185	0.0136
21:15	0.8494	0.8782	0.3396	0
21:30	0.8037	0.8881	0.3181	0
21:45	0.8060	0.9240	0.3138	0
22:00	0.7683	0.8791	0.3078	0

Table 3 Load priorities of 69-bus distribution system

Critical loads	Normal loads
15–29, 30–40, 57–59, 62–65	1–14, 41–56, 60–61

Table 1; each is equipped with an AMI meter. It is assumed that the 40 m are connected via a ring communication network. As discussed in Section 3, for a ring cyber network with 40 m, the second smallest eigenvalue of the corresponding Laplacian matrix is 0.0246 and the 40th smallest (i.e. the largest) one is 4.0. Therefore, the step size is $\tau = 2/[\varphi_2(L) + \varphi_{40}(L)] = 0.4969$.

Table 4 Service restoration with and without MGs

|	Fault location	Switch status	Restored load (bus number)	Restored load, kW[a]	On-outage load, kW[a]	
with MGs	6–7, 18–19, 22–23, 28–29, 56–57, 61–62	close 15–46 and 50–59	7, 8, 9, 10, 11, 12, 13, 14, 15, 16, 17, 18, 19, 20, 21, 22, 23, 24, 25, 26, 27, 29, 30, 31, 32, 33, 34, 35, 51, 52, 53, 54, 55, 56, 57, 58, 59, 60, 61, 62, 63, 64, 65, 66, 67, 68, 69	2739.7	0	additional buses (bus number) restored with MGs
without MGs	6–7, 18–19, 22–23, 28–29, 56–57, 61–62	close 13–21, 15–46 and 50–59	7, 8, 9, 10, 11, 12, 13, 14, 15, 16, 17, 18, 19, 20, 21, 22, 51, 52, 53, 54, 55, 56, 57, 58, 59, 60, 61, 66, 67, 68, 69	2300.2	439.5	23, 24, 25, 26, 27, 29, 30, 31, 32, 33, 34, 35, 62, 63, 64, 65

[a] At peak time 17:15
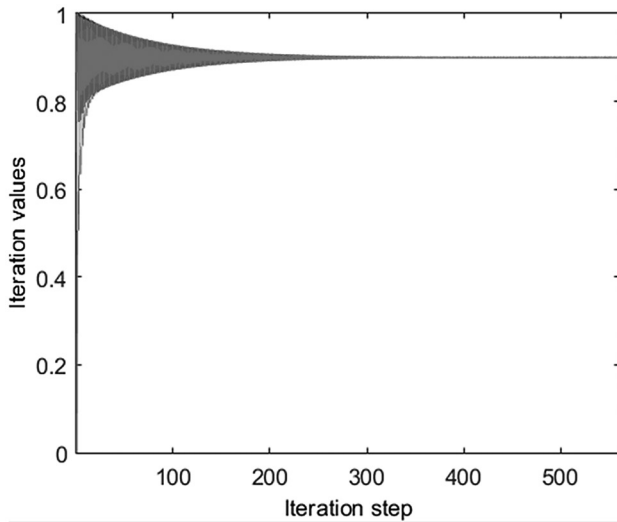
Fig. 5 *Convergence of connection status of AMI meters at bus 21*
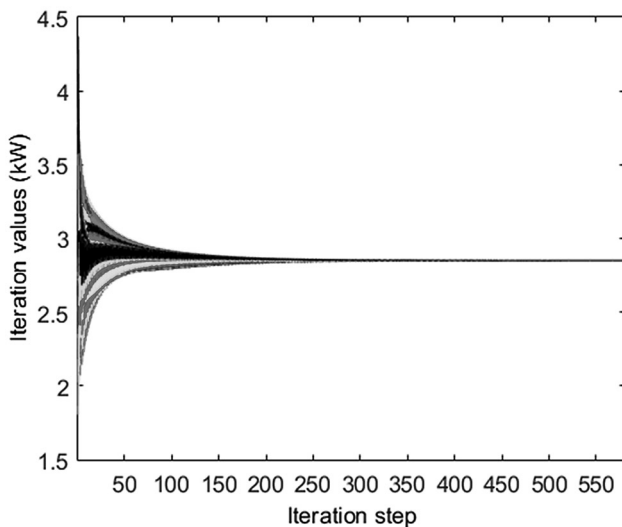
Fig. 6 *Convergence of AMI-meter readings at bus 21*

Fig. 5 shows the iteration of $\bar{\gamma}$ at 17:15 for AMI meters at bus 21. We assume that there are 36 loss-of-power meters, i.e. the initial states of 36 m are one and 4 m are zero. At the end, the algorithm converges to 0.9. The routing meter knows that there are 36 out-of-service meters by using (2). Fig. 6 presents the convergence of meter readings. Each meter starts the iteration with its own active power, which is randomly assigned and exchanges information with its neighbouring meters in the ring-connected cyber network. The algorithm converges to the same value 2.85 kW, which is the averaged load of all customers. At the beginning, each meter only

Table 5 Output (kilowatts) of MTs at 17:15

MT number	Output, kW	MT number	Output, kW
MT 8[a]	120.32	MT 29	185.03
MT 11	120.32	MT 39	120.32
MT 12	120.32	MT 45	120.32
MT 16	120.32	MT 48	120.32
MT 21	245.23	MT 62	245.05
MT 27	178.12	MT 64	245.06

[a]MT 8 represents the MT in the MG integrated at bus 8 in the primary distribution system

Table 6 Output (kilowatts) of ESS at 17:15

ESS number	Output, kW	ESS number	Output, kW
ESS 8[a]	47.41	ESS 29	48.11
ESS 11	47.41	ESS 39	47.41
ESS 12	47.41	ESS 45	47.41
ESS 16	47.41	ESS 48	47.41
ESS 21	48.90	ESS 62	48.9
ESS 27	46.30	ESS 64	48.9

[a]ESS 8 represents the ESS in the MG integrated at bus 8 in the primary distribution system

Table 7 Output (kilowatts) of MT 21 from 17:15 to 22:00

Time	Output, kW	Time	Output, kW
17:15	245.23	19:45	225.44
17:30	244.92	20:00	220.61
17:45	248.02	20:15	251.32
18:00	247.29	20:30	237.87
18:15	244.52	20:45	246.61
18:30	231.07	21:00	245.98
18:45	236.42	21:15	239.65
19:00	244.07	21:30	245.97
19:15	230.08	21:45	246.27
19:30	221.83	22:00	244.68

knows its own load; at the end, the routing meter knows that the total active load of all customers at this point in time is 114 kW by (4). The convergence time for this ring network with 40 m is 0.089 s. To demonstrate the convergence of a larger system, we also test a ring network with 400 m, and the time is 1.241 s.

After detecting the faults, MG-aided optimal service restoration is performed according to Section 4. Table 5 presents the service restoration plans with and without MGs (only peak-time results are shown). By setting the generation and loads in (17) and (18) to be zero, we can simulate the case without MGs. It can be seen that if there is no MG, only partial load can be restored. In contrast, the MG-aided plan can achieve full load restoration with less switch operations.

Tables 5 and 6 show the active power outputs of MTs and ESSs in MGs, respectively. The MTs in MGs connected with buses 21, 27, 62 and 64 have larger power output. This is because the multiple
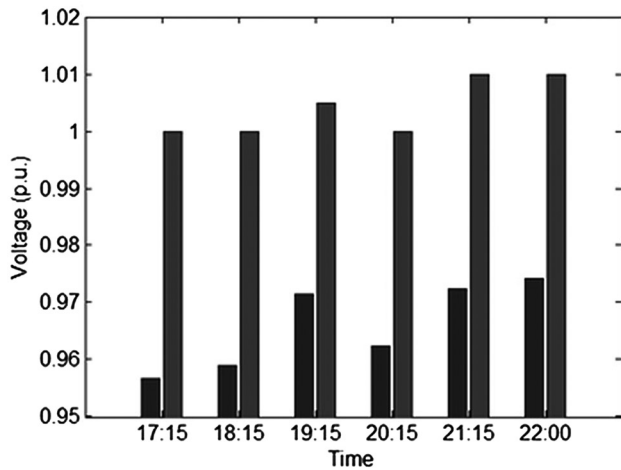
Fig. 7 *Lowest and highest voltage levels from 17:15 to 22:00*

faults make sections 29–35, 19–22, 23–27 and 62–65 islanded from the distribution system. These islanded sections need the power support from MGs to be restored. On the other hand, other on-outage areas can be fully restored by reconfiguration. Table 7 shows the active power output of MT 21 during the outage period. The dispatch of the MT is changing with the load consumption in the distribution system and the MG. About 60 and 20 kW normal load is shed in MGs connected with bus 62 and bus 64, respectively, to fully restore the critical loads in buses 62–65. No other load shedding is necessary since there is enough capacity from MGs and tie switches. The above results demonstrate the effectiveness of using both tie switches and local capacities of MGs to perform the service restoration.

Fig. 7 shows the lowest and highest voltages in the primary distribution system during the outage period. It can be seen that the lowest and highest voltage levels are always within the safe range (±5%) [29].

5 Conclusion

In this paper, we have proposed a method incorporating AMI-based outage detection and MG-aided service restoration. By local information exchanges among AMI meters (i.e. each AMI only exchanges information with its neighbouring counterparts), the total number of on-outage customers and their aggregated last-read power consumption can be obtained in a decentralised fashion. The optimal service restoration based on both traditional reconfiguration and local support from MGs is then performed to maximise the picked-up loads. Simulation results with multiple faults in a severe weather event demonstrate the effectiveness of the proposed technique. Compared with previous effort on FLISR, the proposed method is faster and more resilient since it takes advantage of local capacities of MGs and does not require a centralised communication network. In practical implementation of the proposed method, the renewable DGs such as wind turbines and solar panels are non-dispatchable, and they maybe affected by the extreme weather. Therefore, more dispatchable-DGs such as micro-turbines and diesel generators should be added in the planning stage to enhance the resilience of power systems.

6 Acknowledgment

7 References

1 Ling, W., Liu, D., Lu, Y., *et al.*: 'IEC 61850 model expansion toward distributed fault localization, isolation, and supply restoration', *IEEE Trans. Power Deliv.*, 2014, **29**, (3), pp. 977–984
2 Liu, Y., Schulz, N.N.: 'Knowledge-based system for distribution system outage locating using comprehensive information', *IEEE Trans. Power Syst.*, 2002, **17**, (2), pp. 451–456
3 Chen, S.J., Zhan, T.S., Huang, C.H., *et al.*: 'Nontechnical loss and outage detection using fractional-order self-synchronization error-based fuzzy petri nets in micro-distribution systems', *IEEE Trans. Smart Grid*, 2015, **6**, (1), pp. 411–420
4 Miu, K.N., Chiang, H.-D., McNulty, R.J.: 'Multi-tier service restoration through network reconfiguration and capacitor control for large-scale radial distribution networks', *IEEE Trans. Power Syst.*, 2000, **15**, (3), pp. 1001–1007
5 Toune, S., Fudo, H., Genji, T., *et al.*: 'Comparative study of modern heuristic algorithms to service restoration in distribution systems', *IEEE Trans. Power Deliv.*, 2002, **17**, (1), pp. 173–181
6 Chao-Shun, C., Chia-Hung, L., Hung-Ying, T.: 'A rule-based expert system with colored Petri net models for distribution system service restoration', *IEEE Trans. Power Syst.*, 2002, **17**, (4), pp. 1073–1080
7 Seong-Il, L., Seung-Jae, L., Myeon-Song, C., *et al.*: 'Service restoration methodology for multiple fault case in distribution systems', *IEEE Trans. Power Syst.*, 2006, **21**, (4), pp. 1638–1644
8 Kumar, Y., Das, B., Sharma, J.: 'Multiobjective, multiconstraint service restoration of electric power distribution system with priority customers', *IEEE Trans. Power Deliv.*, 2008, **23**, (1), pp. 261–270
9 Wang, Z., Chen, B., Wang, J., *et al.*: 'Decentralized energy management system for networked microgrids in grid-connected and islanded modes', *IEEE Trans. Smart Grid*, 2016, **7**, (2), pp. 1097–1105
10 Wang, Y., Chen, C., Wang, J., *et al.*: 'Research on resilience of power systems under natural disasters – a review', *IEEE Trans. Power Syst.*, 2016, **31**, (2), pp. 1604–1613
11 Li, J., Ma, X.-Y., Liu, C.-C., *et al.*: 'Distribution system restoration with microgrids using spanning tree search', *IEEE Trans. Power Syst.*, 2014, **29**, (6), pp. 3021–3029
12 Wang, Z., Wang, J.: 'Self-healing resilient distribution systems based on sectionalization into microgrids', *IEEE Trans. Power Syst.*, 2015, **30**, (6), pp. 3139–3149
13 Moreira, C., Resende, F., Peas Lopes, J.: 'Using low voltage microgrids for service restoration', *IEEE Trans. Power Syst.*, 2007, **22**, (1), pp. 395–403
14 Chen, C., Wang, J., Qiu, F., *et al.*: 'Resilient distribution system by microgrids formation after natural disasters', *IEEE Trans. Smart Grid*, 2016, **7**, (2), pp. 958–966
15 Wang, Z., Chen, B., Wang, J., *et al.*: 'Networked microgrids for self-healing power systems', *IEEE Trans. Smart Grid*, 2016, **7**, (1), pp. 310–319
16 Ansari, B., Mohagheghi, S.: 'Electric service restoration using microgrids'. 2014 IEEE PES General Meeting, 2014, pp. 1–5
17 Dominguez-Garcia, A.D., Hadjicostis, C.N.: 'Distributed algorithms for control of demand response and distributed energy resources'. 2011 50th IEEE Conf. on Decision and Control and European Control Conf. (CDC-ECC), 2011, pp. 27–32
18 Dominguez-Garcia, A.D., Hadjicostis, C.N., Vaidya, N.F.: 'Resilient networked control of distributed energy resources', *IEEE J. Sel. Areas Commun.*, 2012, **30**, (6), pp. 1137–1148
19 EEI: 'Smart meters and smart meter systems: a metering industry perspective', 2011. Available at http://www.eei.org/issuesandpolicy/grid-enhancements/documents/smartmeters.pdf
20 Chen, C., Wang, J., Kishore, S.: 'A distributed direct load control approach for large-scale residential demand response', *IEEE Trans. Power Syst.*, **PP**, pp. 1–10, 2014, **29**, (5), pp. 2219–2228
21 Baran, M.E., Wu, F.F.: 'Network reconfiguration in distribution systems for loss reduction and load balancing', *IEEE Trans. Power Deliv.*, 1989, **4**, (2), pp. 1401–1407
22 Taylor, J.A., Hover, F.S.: 'Convex models of distribution system reconfiguration', *IEEE Trans. Power Syst.*, 2012, **27**, (3), pp. 1407–1413
23 Yeh, H.-G., Gayme, D.F., Low, S.H.: 'Adaptive VAR control for distribution circuits with photovoltaic generators', *IEEE Trans. Power Syst.*, 2012, **27**, (3), pp. 1656–1663
24 Khodaei, A.: 'Microgrid optimal scheduling with multi-period islanding constraints', *IEEE Trans. Power Syst.*, 2014, **29**, (3), pp. 1383–1392
25 Derakhshandeh, S.Y., Masoum, A.S., Deilami, S., *et al.*: 'Coordination of generation scheduling with PEVs charging in industrial microgrids', *IEEE Trans. Power Syst.*, 2013, **28**, (3), pp. 3451–3461
26 Grossmann, I.E., Viswanathan, J., Vecchietti, A., *et al.*: 'GAMS/DICOPT: a discrete continuous optimization package', *Math. Methods Appl. Sci.*, 2001, **24**, (11), pp. 649–664
27 Savier, J.S., Das, D.: 'Impact of network reconfiguration on loss allocation of radial distribution systems', *IEEE Trans. Power Deliv.*, 2007, **22**, (4), pp. 2473–2480
28 Zidan, A., El-Saadany, E.F.: 'A cooperative multiagent framework for self-healing mechanisms in distribution systems', *IEEE Trans. Smart Grid*, 2012, **3**, (3), pp. 1525–1539
29 ANSI: 'ANSI standard C84.1-1995 electric power systems and equipment voltage ratings (60 Hz)', 1995